Asian Journal of Chemistry; Vol. 37, No. 5 (2025), 1105-1110

ASIAN JOURNAL OF CHEMISTRY

https://doi.org/10.14233/ajchem.2025.33658

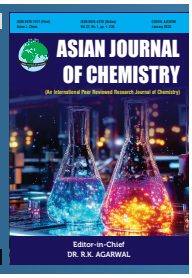

Synthesis, Characterization, Antioxidant and Cytotoxicity Studies of Biogenic Silver Nanoparticles Derived from *Vitex negundo* Leaves

SIVAKUMAR RAMALINGAM and RENUKA SARAVANAN*

Department of Chemistry and Biosciences, SASTRA Deemed to be University, Srinivasa Ramanujan Centre, Kumbakonam-612001, India

*Corresponding author: E-mail: renuka@src.sastra.edu

Received: 11 February 2025; *Accepted*: 29 March 2025; *Published online*: 30 April 2025; AJC-21976

In the current study, the green synthesis of silver nanoparticles from *Vitex negundo* leaves was subjected to antioxidant and anticancer activities. Characterization of silver nanoparticles using techniques like particle size, FTIR, SEM and UV-Vis spectroscopy were analyzed. SEM results indicate that the silver nanoparticles have an average diameter of 130 nm and exhibit a rod-shaped morphology. The UV-visible absorption peak in the 458.35-398.75 nm region is indicative of silver nanoparticles and signifies the presence of surface plasmon resonance. The presence of silver nanoparticles can lead to sharper and more intense absorption peaks in the FTIR spectrum. Silver nanoparticles can enhance the antioxidant properties of *Vitex negundo* with an IC_{50} value of 172.76 µg/mL. Similarly, thiobarbituric acid assay exhibits 100 µg/mL, hydrogen peroxide exhibits 146.68 µg/mL and reducing power assay displays 150 µg/mL. The cytotoxic effects of AgNPs were assessed using the MTT assay on MCF-7 cells. The calculated IC_{50} value was found to be 128.62 µg/mL, suggesting that AgNPs exhibit dose-dependent cytotoxicity. Findings of AO/EtBr assay are useful for understanding the cytotoxic effects of green-synthesized silver nanoparticles. Based on this, successful synthesis of AgNPs from *Vitex negundo*, highlighting their antioxidant and anticancer potential.

Keywords: Green synthesis, Silver nanoparticles, Antioxidant, Anticancer, MCF-7cell line.

INTRODUCTION

Vitex negundo, often referred to as the Chinese chaste tree, five-leaved chaste tree or horseshoe vitex, is a large aromatic shrub belonging to the Lamiaceae family. This plant is widely utilized in traditional medicine, particularly in South and Southeast Asia [1]. Traditionally, *Vitex negundo* is used to relieve pain and inflammation linked to conditions like arthritis and joint pain. It is also effective in managing respiratory issues such as asthma and bronchitis and treating skin infections and wounds [1]. Furthermore, it supports digestive health and helps regulate menstrual cycles, making it a cherished remedy in Ayurvedic medicines [2].

Breast cancer is currently one of the most prevalently diagnosed cancers and the 5th cause of cancer-related deaths with an estimated number of 2.3 million new cases worldwide according to the GLOBOCAN 2020 data [3]. The etiology of breast cancer is multifactorial, involving a complex interplay of genetic, environmental, hormonal and lifestyle factors [4]. Conventional breast cancer therapies including surgery, radiation therapy, chemotherapy and hormonal treatments, are essential for managing the disease but often come with various side effects. Nanoparticles can deliver drugs directly to the tumor cells with high precision, bypassing healthy tissues and reducing the systemic toxicity [5].

Silver nanoparticles (AgNPs) have garnered significant attention due to their exceptional physico-chemical properties, including antimicrobial, antioxidant and catalytic activities [6-9]. The eco-friendly approach leverages the plant's rich content of biologically active compounds, such as flavonoids, polyphenols and terpenoids, which act as reducing and stabilizing agents [10]. Recent studies have highlighted the potential of AgNPs synthesized using *V. negundo* leaf extract for their anticancer properties [6,10]. These nanoparticles have shown promising results in inhibiting the proliferation of cancer cells, such as HepG2 cells, in a dose- and duration-dependent manner [11,12]. Understanding these potential adverse effects can help patients and caregivers prepare and manage them effectively

[13]. Hence, the main aim of this work is to synthesize biogenic AgNPs from *Vitex negundo* leaves and to assess its cytotoxic effect against breast cancer cell line MCF-7.

EXPERIMENTAL

The *Vitex negundo* fresh leaves were collected from the surrounding areas of Kudavasal (10º52′20″N 79º29′09″E), Thiruvarur District, India and authenticated by the Botanist, SASTRA University, Kumbakonam, India. It was air-dried in a shaded room for 16 days and then crushed into a fine powder. The dried plant material was stored in a plastic bag in a refrigerator until further extraction. All the chemicals and reagents were of analytical grade and procured from HiMedia (Mumbai, India).

Preparation of leaf powder: The *V. negundo* leaves were cleaned thoroughly with sterile distilled water, diced into small pieces and shade dried for two weeks at room temperature. Finally, the leaves were ground into a coarse powder using a mechanical blender, then placed in an airtight container for further examination.

Preparation of plant extract: To prepare the extract, 100 mL of distilled water was mixed with 5 g of powdered *V. negundo* leaves. The mixture was then boiled for 25 min at 60 ºC, after which it was allowed to cool to room temperature. The extract was subsequently filtered using Whatman No. 1 filter paper.

Preparation of silver nanoparticles: In a clean glass beaker, slowly added 10 mL of prepared *V. negundo* leaf extract dropwise to 90 mL of freshly prepared silver nitrate solution. The mixture was carefully agitated with a magnetic stirrer and subsequently subjected to mild heating (30-60 ºC) for 24 h. As the reduction process occurs, a colour change from colourless to yellowish-brown, brown or dark brown will typically be observed. This colour change signals the formation of silver nanoparticles, which is due to the surface plasmon resonance phenomenon [14].

Characterization: The biogenic AgNPs were characterized with UV-Vis spectrophotometer (Shimadzu 1800), SEM (VEGA 3 TESCAN), FT-IR (Shimadzu IRAffinity-1S using KBr in the range of 4000-400 cm^{-1}), dynamic light scattering (DLS, Malvern Zetasizer, Malvern Instruments Ltd., Malvern, U.K.) was used to gauge the AgNPs particle size distribution.

Antioxidant assay: The free-radical scavenging activity was assessed using 1,1-diphenyl-2-picrylhydrazyl (DPPH) assay, following a standard procedure [15]. A 0.3 mM DPPH solution in 95% methanol was prepared. A 1 mL of this solution was mixed with 3 mL of biogenic AgNPs and then allowed to stand in dark at room temperature for 30 min. Absorbance was measured at 515 nm using a colorimeter, with the experiment repeated three times. A decrease in the absorbance of DPPH solution indicated an increase in antioxidant activity. The free-radical scavenging activity was expressed as the percentage of inhibition of the DPPH radical. The antioxidant activity was calculated as:

$$\text{Inhibition (\%)} = \frac{\text{Control} - \text{Sample}}{\text{Control}} \times 100$$

Hydrogen peroxide radical scavenging assay: This test was conducted using freshly produced hydrogen peroxide in (PBS) phosphate buffered saline at a pH of 7.4 at different concentrations (50, 100, 150, 200 and 250 µg/mL) of AgNPs. A final volume of 1 mL of phosphate-buffered saline and 600 µL of H_2O_2 (100 mM) were added to each test tube. The preparation of control, which did not include AgNPs, was done using the same manner as previously described. After 10 min, H_2O_2 absorbance at 230 nm was assessed against a blank solution made of phosphate buffer without H_2O_2.

$$\text{Scavenging (\%)} = \frac{\text{Abs}_{\text{control}} - \text{Abs}_{\text{test}}}{\text{Abs}_{\text{blank}}} \times 100$$

Thiobarbituric acid assay: AgNPs samples were taken in test tubes at various concentrations (50, 100, 150, 200 and 250 µg/mL) with ascorbic acid employed as a standard. A 2 mL each of 20% TCA and 0.67% 2-TBA make up the reaction mixture in the test tubes. The sample solution was centrifuged for 20 min at 3000 rpm after cooling in the hot water bath for a short while. The optical density of the supernatant was measured at 552 nm.

$$\text{Scavenging (\%)} = \frac{\text{Abs}_{\text{control}} - \text{Abs}_{\text{test}}}{\text{Abs}_{\text{blank}}} \times 100$$

Reducing power assay: A prepared phosphate buffer, 2.5 mL of $K_4[Fe(CN)_6]$ and 1 mL of AgNPs were combined with concentrations of 50, 100, 150, 200 and 250 µg/mL respectively. Following that, the mixture was incubated for 20 min at 50 ºC. Trichloroacetic acid solution (2.5 mL) was added to stop the process. After that the fluid underwent for 8 min at 3000 rpm centrifugation. After 10 min, 15 mL of distilled water, 15 mL of supernatant solution and 1 mL of $FeCl_3$ solution were mixed. The absorbance was measured at a wavelength of 700 nm. As the absorbance of the reaction mixture increased, it became evident that the reducing capability of the AgNPs had similarly intensified.

$$\text{Scavenging (\%)} = \frac{\text{Abs}_{\text{control}} - \text{Abs}_{\text{test}}}{\text{Abs}_{\text{blank}}} \times 100$$

Anticancer assay

Maintenance of cell: MCF-7 cells were supplied by the National Centre for Cell Science, Pune, India. The cells were grown in a culture flask with 5% CO_2 incubator, 3% L-glutamine, 10% foetal bovine serum, penicillin, streptomycin, amphotericin B and 7.5% sodium bicarbonate. For the number of flasks needed for additional investigation, the cells were passaged.

MTT assay: The cytotoxic effects of biogenic AgNPs on MCF-7 cells were investigated using MTT assay. A seeding density of 5000 cells per well was used to seed cells onto 96-well plates with 100 µL of medium. After that, the plate was incubated with 5% CO_2 at 37 ºC for 24 h to encourage cell adhesion. After 24 h, the used medium was removed from the 96-well plates with the cells already present and 100 µL of fresh medium was added. The cells were then given treatments with nanoparticles in different doses (15.62, 31.35, 62.5, 125, 250 µg/0.1 mL in DMSO) and cultured for an additional 24 h

at 37 ºC and 5% CO_2. The well plate was subjected to three incubation periods, each lasting 24 h, using 20 µL (20 mg/mL) MTT solution. All three incubations occurred at the same time. The formazan crystals were preserved by carefully eliminating the incubation solution; after that, they were dispersed in 100 mL of DMSO and their optical density at 570 nm was measured with an ELISA [16].

$$\text{Cell viability} = \frac{\text{Absorbance of treated cells}}{\text{Absorbance of control cells}} \times 100$$

Acridine orange/ethidium bromide staining: This study set out to assess the efficiency of dual acridine orange/ethidium bromide (AO/EtBr) staining for the detection of tumour cell apoptosis. Six well plates were used to culture MCF-7 cells to a density of 1×10^5 cells per well for 24 h. Cells were then exposed to the calculated inhibitory concentration (IC_{50}) for 24 h. The unexposed cells to AgNPs were taken as control. Cell suspension were washed thrice with PBS and then resuspended in 25 µL of dye mixture (100 µg/mL of acridine orange and 100 µg/mL of ethidium bromide prepared in PBS and mixed gently). Then, 10 µL were placed on a microscopic slide, covered with a cover-slip and examined under 400X magnification using fluorescent microscope [15].

RESULTS AND DISCUSSION

Plants act as reducing agents and contain compounds like polyphenols, flavonoids and terpenoids that facilitate the reduction of silver ions (Ag^+) to form silver nanoparticles (Ag NPs). AgNPs were formed, as evidenced by the development to a reddish-brown colour after 24 h incubation.

UV-visible studies: The UV-VIS was conducted to confirm the formation of AgNPs as a result of the elevated radiation absorption levels uncovered surface plasmon resonance (SPR) peaks at approximately 398.75 nm and 458.35 nm (Fig. 1). In most cases, biogenic AgNPs in aqueous solution absorb light with a wavelength of 430 nm, giving them a reddish-brown appearance [17].

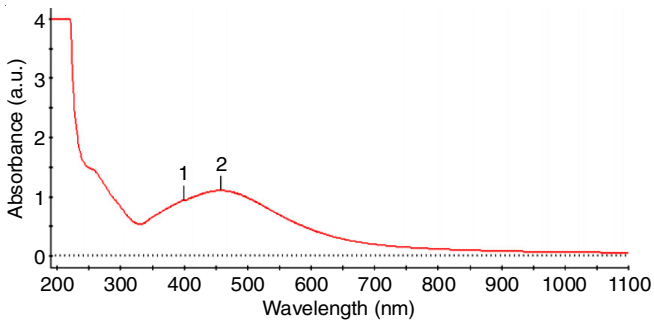

Fig. 1. UV-Vis spectrophotometer analysis of AgNPs

SEM studies: The SEM images of biogenic AgNPs show the spherical-shaped, well-scattered particles with a virtually compact arrangement, with average diameters of 200 nm (Fig. 2).

DLS measurement: According to Fig. 3, the AgNPs are 133 nm in size. The biosynthesized nanoparticles exceeded the intended size range of 1-100 nm. The protein that was attached

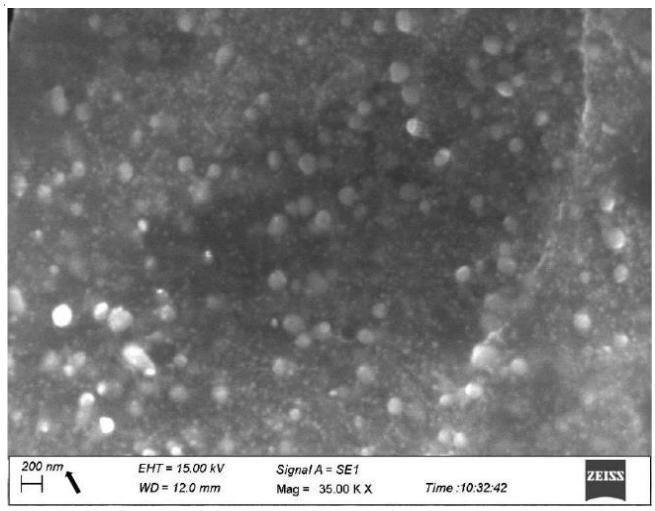

Fig. 2. SEM analysis of AgNPs

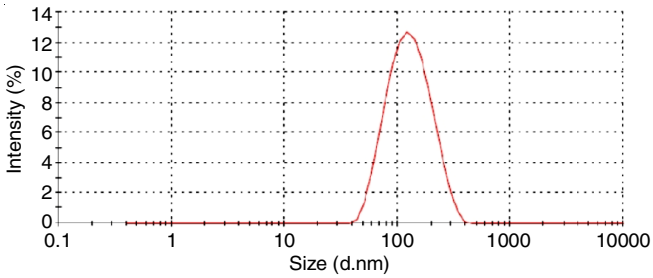

Fig. 3. Zeta size distribution-the peak revealed the size of AgNPs is 133 nm

to the nanoparticles' surface caused their size to be larger than expected [18].

FTIR studies: The silver ion reduction and interaction with AgNPs caused by the biomolecules present in the leaf extract as suggested FTIR analysis. AgNPs have strong IR bands at 3444.91, 2077.99, 1633.84, 1384.48, 1100.96, 1021.03 and 606.91 cm^{-1}. The extensive band at 3444.91 cm^{-1} corresponds to the stretching vibration of (O-H) of phenolic, 2077.99 cm^{-1} indicates the existence of the functional group (N=C=S), 1633.84 cm^{-1} indicates the existence of the functional group (C=C), 1384.48 cm^{-1} indicates the existence of the functional group (C-H), 1100.96 cm^{-1} indicates the existence of the functional group (C-F), 1021.03 cm^{-1} indicates the existence of the functional group (CO-O-CO) and 606.91 cm^{-1} indicates the existence of the functional group (C-Br) (Fig. 4). Thus based on the IR spectra, it may be assumed that these biomolecules play a role in bioreduction as well as biosynthetic stability of silver nanoparticles.

Antioxidant efficiency of silver nanoparticles

DPPH scavenging assay: The results are often plotted as a dose-response curve, showing the relationship between the concentration of AgNPs and the antioxidant activity. The maximum absorption of 65.8% was observed at a concentration of 250 µg/mL. Ascorbic acid was used as reference standard and it displays 70.5% inhibition at 250 µg/mL (Fig. 5). It was determined that the IC_{50} value was 172.76 µg/mL. This data shows that the silver nanoparticles synthesized from *V. negundo* leaf extract may have some free radical scavenging properties.

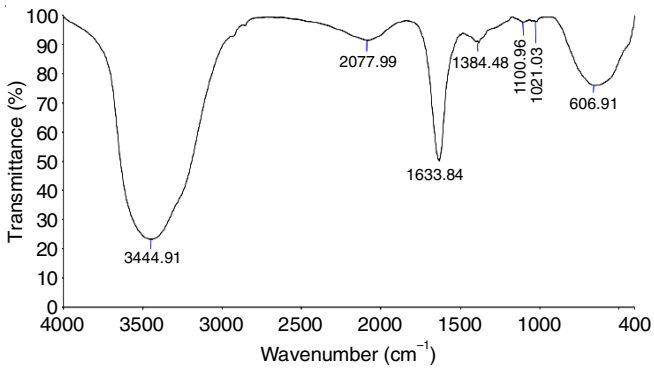

Fig. 4. FTIR spectroscopy analysis revealed the presence of multiple functional groups in AgNPs

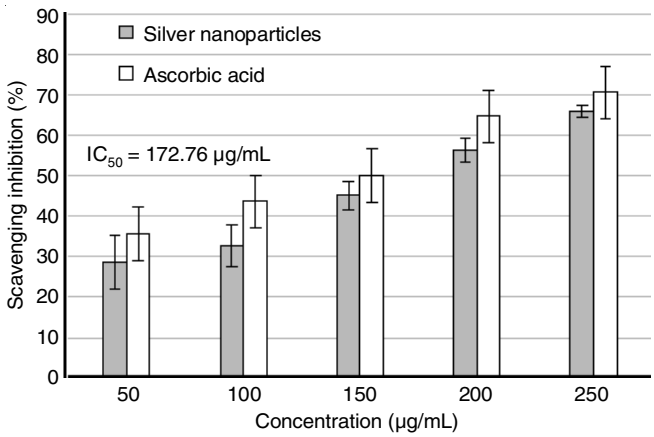

Fig. 5. Antioxidant activity of AgNPs from *Vitex negundo* by DPPH assay

As the concentration of AgNPs increases, the % inhibition of the DPPH radical also increases indicating that AgNPs exhibit antioxidant properties.

Hydrogen peroxide radical scavenging activity: In this assay, AgNPs can act as antioxidants by scavenging hydrogen peroxide (H_2O_2), a reactive oxygen species (ROS), thus protecting cells and tissues from oxidative damage. Fig. 6 illustrates the highest absorption of 65% at 250 µg/mL. Ascorbic acid is used as the standard in this case and at 250 µg/mL, it shows 70% inhibition. The result was determined to be 146.68 µg/mL. Several studies have shown that AgNPs possess the ability

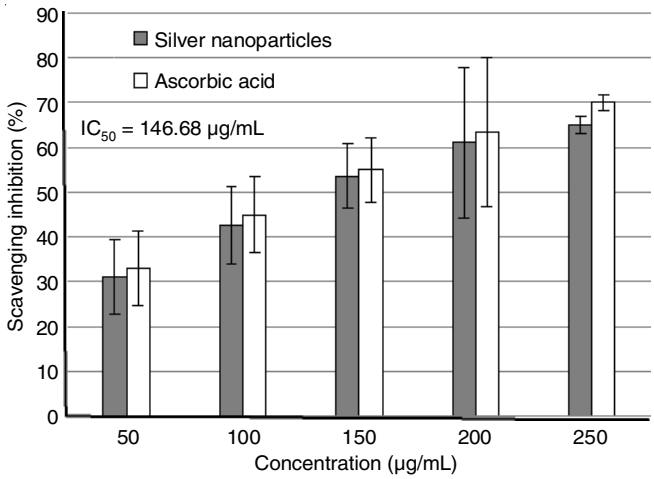

Fig. 6. Antioxidant activity of AgNPs from *Vitex negundo* by H_2O_2 assay

to neutralize reactive species through various mechanisms, including electron donation or hydrogen atom transfer, breaking down H_2O_2 into water and oxygen [19].

Reducing power assay: As AgNPs concentration rises, so does the proportion of inhibition. There is a 70% maximum absorption at 250 µg/mL. Ascorbic acid is used in this instance as the standard and at 250 µg/mL, it displays 75% inhibition (Fig. 7). The determined IC_{50} value was 150 µg/mL and confirmed that the AgNPs synthesized from *V. negundo* leaf extract may be able to scavenge the free radicals.

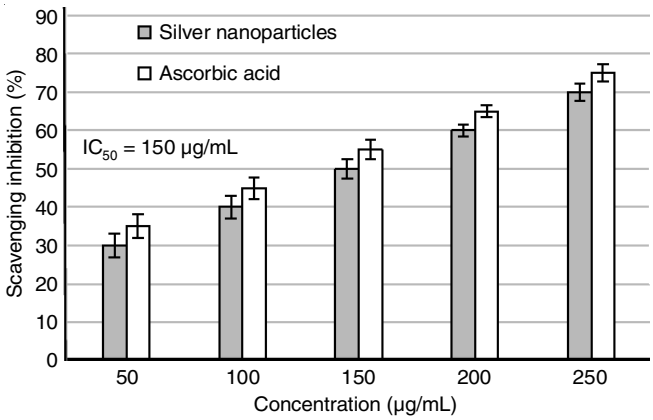

Fig. 7. Antioxidant activity of AgNPs from *Vitex negundo* by reducing power assay

Thiobarbituric acid assay: In this method, the proportion of inhibition increases along with the AgNPs concentration. Fig. 8 illustrates the maximum absorption, which is 80% at 250 µg/mL. The standard utilized in this instance is ascorbic acid, which exhibits a 70% inhibition at a dose of 250 µg/mL. The IC_{50} value was found to be as 100 µg/mL. As a result, the AgNPs created from *V. negundo* leaf extract may have potential free radical scavenging action.

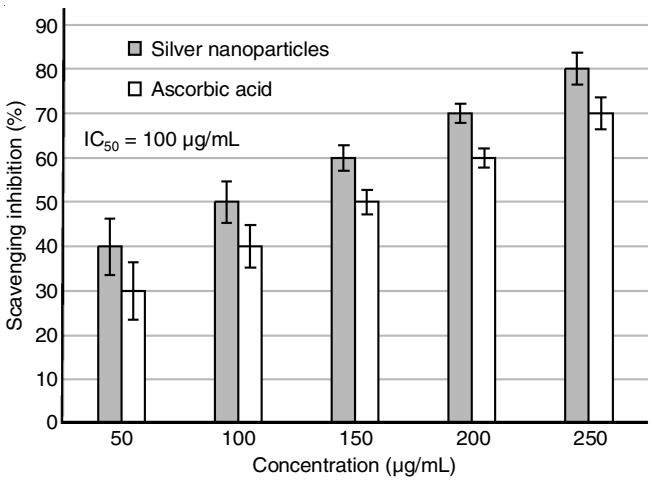

Fig. 8. Antioxidant activity of AgNPs from *Vitex negundo* by thiobarbituric acid assay

In vitro anticancer activities

MTT assay: The MCF-7 cell line was exposed to various concentrations of AgNPs (15.625, 31.25, 62.5, 125 and 250

µg/mL) to assess cell viability. As shown in Fig. 9, the treatment with AgNPs resulted in a significant reduction in cell viability in a concentration-dependent manner. The IC_{50} value for AgNPs in MCF-7 cells was determined to be 128.62 µg/mL. The anticancer mechanism of silver nanoparticles (AgNPs) involves their entry into cells, where they either form a stable S-Ag bond with an enzyme's thiol group, inactivating the enzyme or disrupt hydrogen bonds between nitrogen bases in DNA, causing denaturation [20]. Overall, the biosynthesized AgNPs have been shown to exhibit low or no toxicity to normal cells, while demonstrating broad efficacy against cancer cells in a concentration-dependent manner. The results of this study align with findings from other research that demonstrates the anticancer effect of AgNPs synthesized from *V. negundo* leaves extract on a breast cancer cell line.

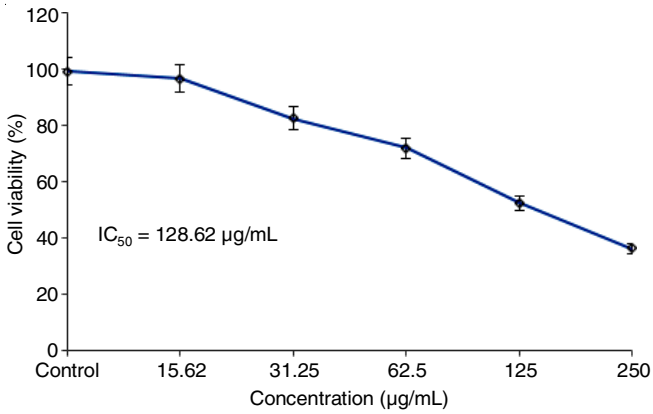

Fig. 9. Cytotoxicity assay of AgNPs from *Vitex negundo*

Acridine orange/ethidium bromide staining: The presence of highly structured green-fluorescing nuclei indicated viable and healthy cells. Apoptotic cells were characterized by reddish-orange fluorescing nuclei, while necrotic cells exhibited swollen, red-fluorescing nuclei. The apoptotic and necrotic changes in MCF-7 cells after treatment are shown in Fig. 10, while the untreated (control) cells, which displayed no signs of apoptosis. By comparing the fluorescence patterns between treated and

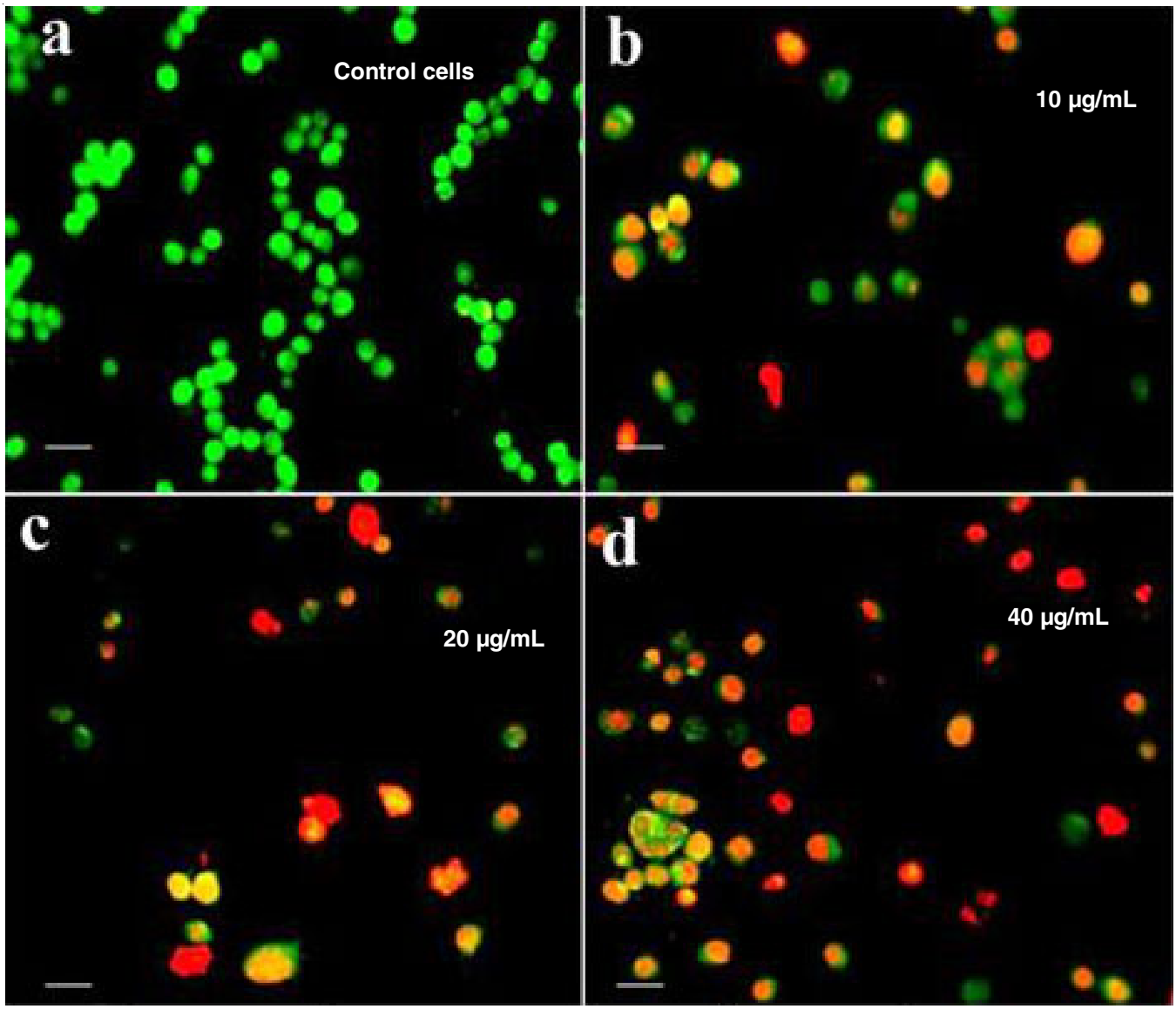

Fig. 10. Apoptotic induction effect of AgNPs from *Vitex negundo* on MCF-7 cells (AO/EtBr)

untreated groups, the AO/EtBr assay helps demonstrate the apoptotic and necrotic effects of AgNPs from *V. negundo* on MCF-7 cells. The treated cells may show a higher proportion of apoptotic or necrotic cells, indicating the cytotoxic activity of the AgNPs. Many workers reported that AO/EtBr untreated MCF-7 cells (control) did not exhibit any significant adverse effects compared to cells treated with the active fractions present in plant extract. However, a concentration-dependent increase in the apoptotic effect was observed, which was significant in the treated cell [21]. Additionally, AO/EtBr staining is capable of detecting mild DNA damage. Based on this, the AO/EtBr assay provides strong evidence of the apoptotic and necrotic effects of AgNPs from *V. negundo* leaves extract on MCF-7 cells, supporting their potential as a promising anticancer agent.

Conclusion

In this work, AgNPs synthesized from *Vitex negundo* leaves extract, where the plant extract acted as both a reducing and stabilizing agent, facilitating the conversion of silver ions into nanosized particles with significant stability. The biogenic AgNPs were characterized by various techniques, including UV-vis spectroscopy, scanning electron microscopy (SEM) and Fourier-transform infrared spectroscopy (FTIR), which confirmed their size, shape and chemical composition. The MTT assay results for AgNPs synthesized from *V. negundo* leaves demonstrated a significant concentration-dependent cytotoxic effect on MCF-7 breast cancer cells. The treatment with these biogenic nanoparticles led to a remarkable reduction in cell viability, indicating their potent anticancer activity. The results from the antioxidant assay further support the therapeutic potential of AgNPs from *V. negundo,* as only exhibit protective benefits against oxidative damage. The calculated IC_{50} value of 128.62 µg/mL, suggesting that AgNPs exhibit dose-dependent cytotoxicity. The AgNPs induced significant apoptotic and necrotic cell death, as observed through various assays, including the AO/EtBr assay, which highlighted early and late apoptosis as well as necrosis. Overall, this study provides compelling evidence that AgNPs synthesized from *V. negundo* leaves possess significant anticancer potential, making them a promising candidate for future cancer therapies. However, further *in vivo* studies, along with clinical evaluations, are necessary to fully understand the mechanisms of action, toxicity profiles and therapeutic efficacy of these nanoparticles in cancer treatment.

CONFLICT OF INTEREST

The authors declare that there is no conflict of interests regarding the publication of this article.

REFERENCES

1. S. Perveen, M.A. Khan, R. Parveen, A. Insaf, B. Parveen, S. Ahmad and S.A. Husain, *Curr. Tradit. Med.*, **9**, e270822208079 (2023); https://doi.org/10.2174/2215083808666220827115915
2. B.S. Gill, R. Mehra, Navgeet and S. Kumar, *Mol. Biol. Rep.*, **45**, 2925 (2018); https://doi.org/10.1007/s11033-018-4421-3
3. E.T. Sedeta, B. Jobre and B. Avezbakiyev, *J. Clin. Oncol.*, **41**, 16S (2023); https://doi.org/10.1200/JCO.2023.41.16_suppl.10528
4. P.A. Fasching, A.B. Ekici, B..R. Adamietz, D.L. Wachter, A. Hein, C.M. Bayer, L. Häberle, C.R. Loehberg, S.M. Jud, K. Heusinger, M. Rübner, C. Rauh, M.R. Bani, M.P. Lux, R. Schulz-Wendtland, A. Hartmann and M.W. Beckmann, *Geburtshilfe Frauenheilkd*, **71**, 1056 (2011); https://doi.org/10.1055/s-0031-1280437
5. S. Ajith, F. Almomani, A. Elhissi and G.A. Husseini, *Heliyon*, **9**, e21227 (2023); https://doi.org/10.1016/j.heliyon.2023.e21227
6. A.S. Rodrigues, J.G.S. Batista, M.Á.V. Rodrigues, V.C. Thipe, L.A.R. Minarini, P.S. Lopes amd A.B. Lugão, *Front. Microbiol.*, **15**, 1440065 (2024); https://doi.org/10.3389/fmicb.2024.1440065
7. B. Ahmed, M.B. Tahir, M. Sagir and M. Hassan, *Mater. Sci. Eng. B*, **301**, 117165 (2024); https://doi.org/10.1016/j.mseb.2023.117165
8. T.S. Rashid, Y. Galali, H.K. Awla and S.M. Sajadi, *Results Chem.*, **11**, 101849 (2024); https://doi.org/10.1016/j.rechem.2024.101849
9. B. Sharma, I. Singh, S. Bajar, S. Gupta, H. Gautam and P. Kumar, *Indian J. Microbiol.*, **60**, 468 (2020); https://doi.org/10.1007/s12088-020-00889-0
10. M.M. Shanwaz and P. Shyam, *NanoBioSci.*, **12**, 59 (2022); https://doi.org/10.33263/LIANBS122.059
11. A.A.H. Abdellatif, M.A.H. Mostafa, H. Konno and M.A. Younis, *3 Biotech.*, **14**, 274 (2024); https://doi.org/10.1007/s13205-024-04118-z
12. A. Almatroudi, *Open Life Sci.*, **15**, 819 (2020); https://doi.org/10.1515/biol-2020-0094
13. C. Tommasi, R. Balsano, M. Corianò, B. Pellegrino, F. Bardanzellu, G. Saba, N. Denaro, M. Ramundo, I. Toma, A. Fusaro, S. Martella, M.M. Aiello, M. Scartozzi, A. Musolino and C. Solinas, *J. Clin. Med.*, **11**, 7239 (2022); https://doi.org/10.3390/jcm11237239
14. M. Mani, R. Harikrishnan, P. Purushothaman, S. Pavithra, P. Rajkumar, S. Kumaresan, D.A. Al Farraj, M.S. Elshikh, B. Balasubramanian and K. Kaviyarasu, *Environ. Res.*, **202**, 111627 (2021); https://doi.org/10.1016/j.envres.2021.111627
15. S. Mariyappan, S. Ramalingam, L. Murugan and R. Saravanan, *J. Exp. Biol. Agric. Sci.*, **9**, 678 (2021); https://doi.org/10.18006/2021.9(5).678.686
16. B. Singh, H. Singh, S. Kaur and S. Arora, *Pharmacogn. Mag.*, **16**, 221 (2020); https://doi.org/10.4103/pm.pm_236_19
17. M. Rao and N.K. Kamila, *Karbala Int. J. Mod. Sci.*, **4**, 86 (2017); https://doi.org/10.1016/j.kijoms.2017.11.001
18. A. Roy, *Res. Rev. Biosci.*, **12**, 138 (2017).
19. A.K. Keshari, S. Saxena, G. Pal, V. Srivashtav and R. Srivastav, *Res. J. Biotechnol.*, **16**, 72 (2021); https://doi.org/10.25303/1612rjbt7279
20. S.P. Patil and S.T. Kumbhar, *Biochem. Biophys. Rep.*, **10**, 76 (2017); https://doi.org/10.1016/j.bbrep.2017.03.002
21. R. Saravanan and S. Ramalingam, *J. Chem. Health Risks*, **14**, 235 (2024).